Electronic Research Archive

http://www.aimspress.com/journal/era

ERA, 31(9): 5589–5608.
DOI: 10.3934/era.2023284
Received: 17 June 2023
Revised: 21 July 2023
Accepted: 31 July 2023
Published: 14 August 2023

Research article

Chaos synchronization of stochastic time-delay Lur'e systems: An asynchronous and adaptive event-triggered control approach

Xinling Li[1], Xueli Qin[2], Zhiwei Wan[2] and Weipeng Tai[1,2,*]

[1] Research Institute of Information Technology, Anhui University of Technology, Ma'anshan 243002, China

[2] School of Computer Science & Technology, Anhui University of Technology, Ma'anshan 243032, China

* **Correspondence:** Email: taiweipeng@ahut.edu.cn.

Abstract: We explore the master-slave chaos synchronization of stochastic time-delay Lur'e systems within a networked environment. To tackle the challenges posed by potential mode-mismatch behavior and limited networked channel resources, an asynchronous and adaptive event-triggered (AAET) controller is employed. A criterion on the stochastic stability and $\mathcal{L}_2-\mathcal{L}_\infty$ disturbance-suppression performance of the synchronization-error system is proposed by using a Lyapunov-Krasovskii functional, a Wirtinger-type inequality, the Itô formula, as well as a convex combination inequality. Then, a method for determining the desired AAET controller gains is proposed by decoupling the nonlinearities that arise from the Lyapunov matrices and controller gains. Finally, the applicability of the AAET control approach is validated by a Chua's circuit.

Keywords: Lur'e system; chaos synchronization; asynchronous control; event-triggered control

1. Introduction

Chaotic systems exhibit intricate nonlinear dynamics, characterized by features such as pseudo-random behavior and a heightened sensitivity to initial conditions. Lur'e systems (LSs), which encompass a wide range of chaotic systems such as Chua's circuits [1] neural networks [2], and n-scroll attractors [3], have attracted significant research attention in the past decades. Chaos synchronization of LSs has found applications in diverse areas including image encryption [4–6], cryptography [7, 8] and confidential communication [9–11]. The existence of time delay and stochastic perturbations are often unavoidable in a real-world control system and can cause the system to be unstable. Correspondingly, substantial efforts have been devoted to chaos synchronization of stochastic time-delay LSs, and a few results have been reported [12–15].

When implementing chaos synchronization in a networked environment, network-induced phenomena, such as packet losses [16], link failures [17] and cyber attacks [18–20], can introduce inconsistencies between the system and the controller/filter modes [21]. Therefore, researchers have shown interest in studying chaos synchronization using asynchronous/mode-unmatched controllers. The hidden Markov model (HMM), proposed by Rabiner [22], serves as a suitable tool for describing the asynchronous phenomena. Building upon the HMM framework, Li et al. [23] investigated the synchronization control in Markov-switching neural networks, while Ma et al. [24] explored the drive-response synchronization in fuzzy complex dynamic networks. Despite these advancements, to our knowledge, there is a scarcity of research addressing chaos synchronization in stochastic time-delay LSs under asynchronous controllers.

Moreover, in networked control systems, the bandwidth of the communication network is usually limited, which can impact the control performance significantly. To eliminate unnecessary resource waste and achieve efficient resource allocation, recent studies on chaos synchronization of LSs have utilized event-triggered mechanism (ETM)-based control methods. For instance, Wu et al. [25] conducted research on exponential synchronization and joint performance issues of chaotic LSs by designing a switching ETM based on perturbation terms. He et al. [26] proposed a secure communication scheme through synchronized chaotic neural networks based on quantized output feedback ETM. Besides, several studies on memory-based ETM for chaos synchronization in LSs have been reported in [27–29]. Notably, the above literature employed fixed thresholds in the designed ETM, limiting their ability to conserve communication resources.

Motivated by the above discussion, we explore the master-slave chaos synchronization of stochastic time-delay LSs within an asynchronous and adaptive event-triggered (AAET) control framework. Unlike previous works [25–29], the thresholds of the ETM used can be adjusted adaptively with real-time system states. The objective is to determine the required AAET controller gains to ensure that the synchronization-error system (SES) has both stochastic stability (SS) and $\mathcal{L}_2 - \mathcal{L}_\infty$ disturbance-suppression performance (LDSP) [30]. The contributions of this paper are:

1) The AAET controller is first applied to tackle the chaos synchronization issue of stochastic time-delay LSs;

2) A criterion on the SS and LDSP is proposed using a Lyapunov-Krasovskii functional (LKF), a Wirtinger-type inequality, the Itô formula, as well as a convex combination inequality (CCI);

3) A method for determining the desired AAET controller is proposed by decoupling the nonlinearities that arise from the Lyapunov matrices and controller gains.

2. Preliminaries

Throughout, we employ $\mathbb{R}^{n_1}$, $\mathbb{R}^{n_1 \times n_2}$ and $\mathbb{N}$ to stand for the n_1-dimensional Euclidean space, the set of all $n_1 \times n_2$ real matrices, and the set of natural numbers, respectively. The symbol $\|\cdot\|$ is the Euclidean vector norm, $(\cdot)^T$ represents the matrix transposition, $He(G)$ means the sum of matrix G and its transpose G^T, $*$ indicates the symmetric term in a matrix and $\mathscr{E}\{\cdot\}$ and $Prob\{\cdot\}$ indicate, respectively, the expectation and probability operator. Furthermore, we utilize $col\{\cdot\}$ to denote a column vector, $diag\{\cdot\}$ to stand for a block-diagonal matrix and $\sup\{\cdot\}$ and $\inf\{\cdot\}$ to indicate the supremum and infimum of a set of real numbers, respectively.

2.1. Physical plant

Consider the following master-slave stochastic time-delay LSs:

$$\begin{cases} dx_m(t) = [A_{\alpha(t)}x_m(t) + B_{\alpha(t)}x_m(t-\tau(t)) + W_{\alpha(t)}\psi(Fx_m(t))]\,dt \\ \qquad\qquad +D_{\alpha(t)}x_m(t)d\varpi(t), \\ y_m(t) = C_{\alpha(t)}x_m(t), \\ x_m(t) = \xi_{m0}, t \in [-\tau_2, 0], \end{cases} \tag{2.1}$$

$$\begin{cases} dx_s(t) = [A_{\alpha(t)}x_s(t) + B_{\alpha(t)}x_s(t-\tau(t)) + W_{\alpha(t)}\psi(Fx_s(t)) \\ \qquad\qquad +u(t) + E_{\alpha(t)}v(t)]\,dt + D_{\alpha(t)}x_s(t)d\varpi(t), \\ y_s(t) = C_{\alpha(t)}x_s(t), \\ x_s(t) = \xi_{s0}, t \in [-\tau_2, 0] \end{cases} \tag{2.2}$$

with $x_m(t) \in \mathbb{R}^{n_x}$ and $x_s(t) \in \mathbb{R}^{n_x}$ being the state vectors, ξ_{m0} and ξ_{s0} being the initial values, $y_m(t) \in \mathbb{R}^{n_y}$ and $y_s(t) \in \mathbb{R}^{n_y}$ being the output vectors, $\psi(\cdot) \in \mathbb{R}^q$ being the nonlinear term with all components within $[\acute{g}_r, \grave{g}_r]$ for $r = 1, 2, \cdots, q$, $u(t) \in \mathbb{R}^q$ being the control signal to be designed, $v(t)$ being the disturbance in $L_2[0, \infty)$ [31], one-dimension Brownian motion $\varpi(t)$ satisfying $\mathscr{E}\{d\varpi(t)\} = 0$ and $\mathscr{E}\{d\varpi^2(t)\} = dt$, and time-varying delay $\tau(t)$ satisfying $0 < \tau_1 \leqslant \tau(t) \leqslant \tau_2$ and $\mu_1 \leqslant \dot{\tau}(t) \leqslant \mu_2$, where τ_1, τ_2, μ_1, and μ_2 are constants. $\{\alpha(t), t \geqslant 0\}$ is the Markovian process and belongs to the state space $\mathscr{N} = \{1, 2, \cdots, N\}$. The transition rate (TR) matrix and transition probability is given by $\Pi = [\pi_{ij}]_{N\times N}$ and

$$Prob\,\{\alpha(t+\varsigma) = j|\alpha(t) = i\} = \begin{cases} \pi_{ij}\varsigma + o(\varsigma), i \neq j. \\ 1 + \pi_{ii}\varsigma + o(\varsigma), i = j, \end{cases}$$

with $\varsigma > 0$, $\lim_\varsigma \to 0 o(\varsigma)/\varsigma = 0$, $\pi_{ij} \geqslant 0$, $i \neq j$ and $\pi_{ii} = -\sum_{i=1, i\neq j}^{N} \pi_{ij}$ [32–34]. $A_{\alpha(t)}$, $B_{\alpha(t)}$, $C_{\alpha(t)}$, $D_{\alpha(t)}$, $E_{\alpha(t)}$ and $W_{\alpha(t)}$, which can be abbreviated as A_i, B_i, C_i, D_i, E_i, and W_i for $\alpha(t) = i \in \mathscr{N}$, are matrices with appropriate dimensions.

2.2. Adaptive event-triggered mechanism

In order to minimize information transmission, the adaptive ETM is employed to determine whether the current sampled data should be transmitted to the controller, as illustrated in Figure 1. Let t_kh denote the latest transmission time of the output signal, where $h > 0$ is the sampling period. $y(t_kh)$ and $y(t)$ denote the latest output signal and the current one, respectively. Defining $e(t) = y(t_kh) - y(t)$, the event-triggered condition is designed as follows:

$$t_0h = 0, t_{k+1}h = t_kh + \inf_{p\in\mathbb{N}} \left\{ph|e^T(t)\Psi_i e(t) < \rho(t)y^T(t_kh)\Psi_i y(t_kh)\right\}, t \in [t_kh, t_{k+1}h), \tag{2.3}$$

where $\Psi_i > 0$ is the trigger matrix and $\rho(t)$ is a threshold parameter adjusted by an adaptive law as

$$\rho(t) = \rho_1 + (\rho_2 - \rho_1)\frac{2}{\pi} arccot(\kappa\|e(t)\|^2), \tag{2.4}$$

where ρ_1 and ρ_2 are predetermined parameters with $0 < \rho_1 \leqslant \rho_2 < 1$, κ is a positive scalar used to adjust the sensitivity of the function $\|e(k)\|^2$.

Remark 1. *The value of $\rho(t)$ has a certain influence on the trigger condition (2.3). The trigger condition will be stricter with the value of $\rho(t)$ being higher, resulting in less data being transmitted to the controller. Conversely, the trigger condition will be relaxed with the value of $\rho(t)$ being lower, allowing more data to be transmitted. Furthermore, it is worth to mention that, when $\rho(t)$ takes a constant on* $(0, 1]$*, the adaptive ETM will be transformed into the periodic ETM (PETM); when $\rho(t)$ is set as* 0*, it will be transformed into the sampled-data mechanism (SDM).*

Remark 2. *The arccot function, incorporated in the adaptive law (2.4), enables the threshold parameter of ETM to be dynamically adjusted as the output error changes within the range of* $(\rho_1, \rho_2]$*. The presence of the arccot function results in an inverse relationship between the threshold parameter $\rho(t)$ and the output error $e(t)$. It can be observed that $\rho(t)$ tends to ρ_2 as $||e(t)||^2$ approaches 0, and $\rho(t)$ tends to ρ_1 as $||e(t)||^2$ approaches ∞.*

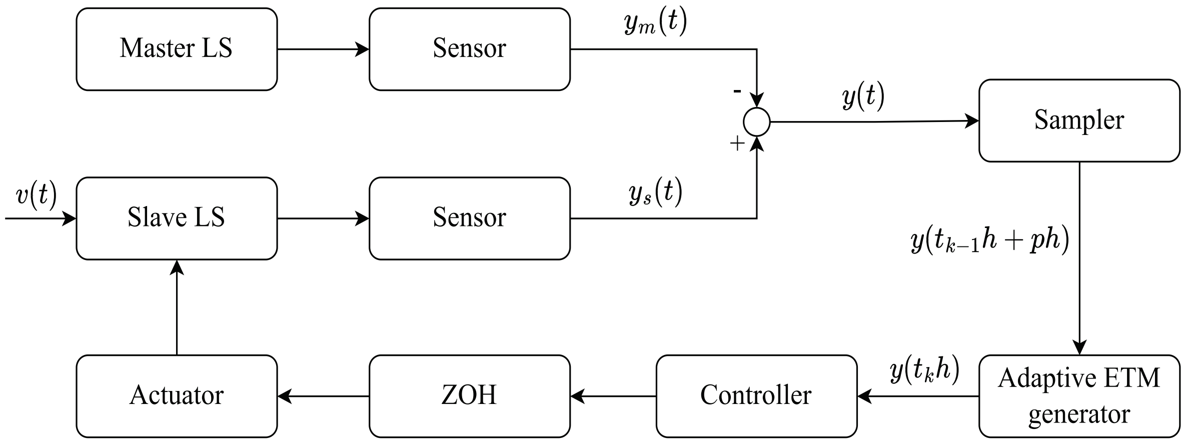

Figure 1. Master-Slave stochastic time-delay LSs.

2.3. Controller

Consider the following controller:

$$u(t) = K_{\beta(t)} \left(y_m(t_k h) - y_s(t_k h)\right), t \in [t_k h, t_{k+1} h). \tag{2.5}$$

Unlike [35–37], the controller is based on output feedback, which is known to be more easily implemented. In the controller, we introduce another stochastic variable with state space $\mathscr{M} = \{1, 2, \cdots, M\}$ to describe this stochastic process $\{\beta(t), t \geqslant 0\}$. The conditional transition probability (CTP) matrix is signed as $\Phi = [\varphi_{i\iota}]_{N\times M}$ with

$$\varphi_{i\iota} = Prob\{\beta(t) = \iota | \alpha(t) = i\}$$

and $\sum_{\iota=1}^{M} \varphi_{i\iota} = 1$. $K_{\beta(t)}$, which will be abbreviated as K_ι, is the controller gain to be designed. Note that $\{\{\alpha(t), t \geqslant 0\}\{\beta(t), t \geqslant 0\}\}$ constitutes a HMM [38, 39].

Define $x(t) = x_m(t) - x_s(t)$. Then, from (2.1), (2.2) and (2.5), one can establish the following SES:

$$dx(t) = \mathscr{F}(t)dt + \mathscr{G}(t)d\varpi(t), t \in [t_k h, t_{k+1} h), \tag{2.6}$$

where $\mathscr{F}(t) = (A_i - K_\iota C_i)x(t) + B_i x(t-\tau(t)) + W_i\tilde{\psi}(Fx(t)) - K_\iota e(t) - E_i v(t)$, $\mathscr{G}(t) = D_i x(t)$, $\tilde{\psi}(Fx(t)) = \psi(F(x(t) + x_s(t))) - \psi(Fx_s(t))$ that satisfies

$$\acute{g}_r \leqslant \frac{\psi_r(f_r^T(x + x_s)) - \psi_r(f_r^T x_s)}{f_r^T x} = \frac{\tilde{\psi}_r(f_r^T x)}{f_r^T x} \leqslant \grave{g}_r, \forall x, x_s, r = 1, 2, \cdots, q, \tag{2.7}$$

where f_r^T indicates the r-th row of F. From (2.7), one can get

$$\left[\tilde{\psi}_r(f_r^T x) - \acute{g}_r f_r^T x\right]\left[\tilde{\psi}_r(f_r^T x) - \grave{g}_r f_r^T x\right] \leqslant 0. \tag{2.8}$$

Remark 3. *The constants $\acute{g}_r$ and $\grave{g}_r$ can be taken as positive, negative, or zero. By allowing $\acute{g}_r$ and $\grave{g}_r$ to have a wide range of values, the sector bounded nonlinearity can flexibly adapt to the needs of different systems and provide a more flexible regulation and control mechanism.*

To streamline the subsequent analysis, we define

$$\begin{aligned}
\zeta(t) &= col\{x(t), x(t-\tau_1), x(t-\tau(t)), x(t-\tau_2), \phi_1, \phi_2, \phi_3\},\\
\varrho_d &= \left[\begin{array}{ccc} 0_{n\times(d-1)n} & I_{n\times n} & 0_{n\times(9-d)n}\end{array}\right](d = 1, 2, \cdots, 9),\\
\phi_1 &= \frac{1}{\tau_1}\int_{t-\tau_1}^{t} x(s)\,ds, \phi_2 = \frac{1}{\tau(t)-\tau_1}\int_{t-\tau(t)}^{t-\tau_1} x(s)\,ds,\\
\phi_3 &= \frac{1}{\tau_2-\tau(t)}\int_{t-\tau_2}^{t-\tau(t)} x(s)\,ds, \tau_{12} = \tau_2 - \tau_1,
\end{aligned}$$

and provide two definitions and four lemmas.

Definition 1. *The SES (2.6) is said to be with SS if there exists a scalar $\mathcal{M}(\alpha_0, \xi(\cdot))$ satisfying*

$$\mathscr{E}\left\{\int_0^\infty \|x(t)\|^2\,dt|\alpha_0, x(t) = \xi_0, t \in [-\tau_2, 0]\right\} < \mathcal{M}(\alpha_0, \xi(\cdot))$$

when $v(t) \equiv 0$.

Definition 2. *Under the zero initial condition, for a given scalar $\gamma > 0$, the SES (2.6) is said to have a LDSP if*

$$\mathscr{E}\left\{\sup_{t\geqslant 0}\{\|y(t)\|^2\}\right\} \leqslant \gamma^2\mathscr{E}\left\{\int_0^t \|v(s)\|^2 ds\right\}$$

holds for $v(t) \neq 0$.

Lemma 1. *Given stochastic differential equation*

$$dx(t) = \mathscr{F}(t)dt + \mathscr{G}(t)d\varpi(t), \tag{2.9}$$

where $\varpi(t)$ is one-dimension Brownian motion, for scalars a, b ($b > a$), and a matrix R, one has

$$\int_a^b \mathscr{F}^T(s)R\mathscr{F}(s)\,ds \geqslant \frac{1}{b-a}\Omega^T(a,b)\tilde{R}\Omega(a,b) + \frac{2}{b-a}\Omega^T(a,b)\tilde{R}\mu(a,b),$$

where $\tilde{R} = diag\{R, 3R\}$ and

$$\Omega(a,b) = \left[\begin{array}{c} x(b) - x(a) \\ x(b) + x(a) - \frac{2}{b-a}\int_a^b x(s)\,ds \end{array}\right], \mu(a,b) = \left[\begin{array}{c} -\int_a^b \mathscr{G}(s)\,d\varpi(s) \\ \frac{1}{b-a}\int_a^b (b+a-2s)\mathscr{G}(s)\,d\varpi(s)\end{array}\right].$$

Remark 4. *Following the approaches used in [40, 41], the Wirtinger-type inequality of Lemma 1 can be readily established. It should be noted that the integral term in* $\mu(a, b)$ *should be* $\frac{1}{b-a}\int_a^b (b+a-2s)\mathscr{G}(s)\, d\varpi(s)$ *instead of* $\frac{1}{b-a}\int_a^b (b-a+2s)\mathscr{G}(s)\, d\varpi(s)$.

Lemma 2. *[40] Consider the stochastic differential equation (2.9). For* $n \times n$ *real matrix* $R > 0$ *and the piecewise function* $\tau(t)$ *satisfying* $0 < \tau_1 \leqslant \tau(t) \leqslant \tau_2$*, where* τ_1 *and* τ_2 *are two constants, and for* $S \in \mathbb{R}_{2n\times 2n}$ *satisfying* $\begin{bmatrix} \tilde{R} & S^T \\ * & \tilde{R} \end{bmatrix} \geqslant 0$ *with* $\tilde{R} = diag\{R, 3R\}$*, the following CCI holds:*

$$-\tau_{12}\int_{t-\tau_2}^{t-\tau_1} \mathscr{F}^T(s)R\mathscr{F}(s)\, ds \leqslant -2\mho_2^T S\mho_1 - \mho_1^T\tilde{R}\mho_1 - \mho_2^T\tilde{R}\mho_2 - 2\wp(d\varpi(t)),$$

where

$$\mho_1 = \Omega(t-\tau(t), t-\tau_1), \mho_2 = \Omega(t-\tau_2, t-\tau(t)),$$
$$\wp(d\varpi(t)) = \frac{\tau_{12}}{\tau(t)-\tau_1}\mho_1^T\tilde{R}\mu(t-\tau(t), t-\tau_1) + \frac{\tau_{12}}{\tau_2-\tau(t)}\mho_2^T\tilde{R}\mu(t-\tau_2, t-\tau(t)).$$

Lemma 3. *[42] For any two matrices* $\mathcal{G}$ *and* $\mathcal{R} > 0$ *with appropriate dimensions,*

$$-\mathcal{G}^T\mathcal{R}^{-1}\mathcal{G} \leqslant \mathcal{R} - \mathcal{G}^T - \mathcal{G}$$

holds true.

Lemma 4. *[43] For a given scalar* $\varepsilon > 0$*, suppose there are matrices* Λ*,* U*,* V *and* W *ensuring*

$$\begin{bmatrix} \Lambda & U+\varepsilon V \\ * & -\varepsilon X - \varepsilon X^T \end{bmatrix} < 0.$$

Then, one gets

$$\Lambda + He(UX^{-1}V^T) < 0.$$

3. Main result

In contrast to the common $\mathcal{H}_\infty$ performance, LDSP imposes a limitation on the energy-to-peak gain from disturbance to the output signal, ensuring it does not exceed a specified disturbance-suppression index [44]. In this paper, we intend to develop an asynchronous controller in (2.5) with the adaptive ETM in (2.3) to guarantee the SS and LDSP of SES (2.6). First, we give a condition to ensure the SS and LDSP of SES (2.6).

Theorem 1. *Given scalars* $\gamma > 0$ *and* ρ_2*, suppose that there exist matrices* $P_i > 0$*,* $Q_1 > 0$*,* $Q_2 > 0$*,* $Q_3 > 0$*,* $R_1 > 0$*,* $R_2 > 0$*,* $\Psi_i > 0$*, diagonal matrix* $L > 0$*, and matrices* S*,* K_ι*, for any* $i \in \mathscr{N}$*,* $\iota \in \mathscr{M}$ *satisfying*

$$\begin{bmatrix} \tilde{R}_2 & S^T \\ * & \tilde{R}_2 \end{bmatrix} \geqslant 0, \tag{3.1}$$

$$C_i^T C_i - P_i < 0, \tag{3.2}$$

$$\Lambda_i = \sum_{c=1}^{M} \varphi_{i\iota} \left(\begin{bmatrix} \Lambda_{i\iota}^{1,1} & \Lambda_i^{1,2} \\ * & -\gamma^2 I \end{bmatrix} + \begin{bmatrix} \tilde{A}_{i\iota}^T \\ -E_i^T \end{bmatrix} \left(\tau_1^2 R_1 + \tau_{12}^2 R_2 \right) \begin{bmatrix} \tilde{A}_{i\iota}^T \\ -E_i^T \end{bmatrix}^T \right) < 0. \tag{3.3}$$

Then the SES (2.6) has the SS and LDSP, where

$$\Lambda_{i\iota}^{1,1} = \begin{bmatrix} \Upsilon_{i\iota}^{1,1} & \Upsilon_i^{1,2} & \Upsilon_{i\iota}^{1,3} \\ * & -He(L) & 0 \\ * & * & (\rho_2 - 1)\Psi_i \end{bmatrix}, \ \Lambda_i^{1,2} = \begin{bmatrix} -\varrho_1^T P_i E_i \\ 0 \\ 0 \end{bmatrix},$$

$$\begin{aligned}
\Upsilon_{i\iota}^{1,1} &= He\left(\varrho_1^T P_i A_{i\iota} - \varrho_1^T F^T \acute{G}^T L \grave{G} F \varrho_1\right) + \varrho_1^T (D_i^T P_i D_i + \tilde{P}_i)\varrho_1 \\
&\quad + \tilde{Q} - 2\mathcal{G}_2^T S \mathcal{G}_1 - \mathcal{G}_0^T \tilde{R}_1 \mathcal{G}_0 - \mathcal{G}_1^T \tilde{R}_2 \mathcal{G}_1 - \mathcal{G}_2^T \tilde{R}_2 \mathcal{G}_2 + \varrho_1^T \rho_2 C_i^T \Psi_i C_i \varrho_1, \\
\Upsilon_i^{1,2} &= \varrho_1^T P_i W_i + \varrho_1^T F^T (\acute{G}^T + F^T) L, \ \Upsilon_{i\iota}^{1,3} = \varrho_1^T \rho_2 C_i^T \Psi_i - \varrho_1^T P_i K_\iota, \\
\tilde{R}_d &= diag\{R_d, 3R_d\}\,(d = 1, 2), \tilde{A}_{i\iota} = \begin{bmatrix} A_{i\iota} & W_i & -K_\iota \end{bmatrix}, \\
\tilde{Q} &= diag\left\{Q_1, -Q_1 + Q_2, (1 - \mu_1)Q_3 - (1 - \mu_2)Q_2, -Q_3, 0_{3n\times 3n}\right\}, \\
A_{i\iota} &= \begin{bmatrix} A_i - K_\iota C_i & 0 & B_i & 0 & 0 & 0 & 0 \end{bmatrix}, \ \tilde{P}_i = \sum_{i=1}^{N} \pi_{ij} P_j, \\
\mathcal{G}_0 &= \begin{bmatrix} \varrho_1 - \varrho_2 \\ \varrho_1 + \varrho_2 - 2\varrho_5 \end{bmatrix}, \mathcal{G}_1 = \begin{bmatrix} \varrho_2 - \varrho_3 \\ \varrho_2 + \varrho_3 - 2\varrho_6 \end{bmatrix}, \mathcal{G}_2 = \begin{bmatrix} \varrho_3 - \varrho_4 \\ \varrho_3 + \varrho_4 - 2\varrho_7 \end{bmatrix}.
\end{aligned}$$

Proof. Select a LKF candidate as:

$$V(t, x(t), \alpha(t), \beta(t)) = \sum_{k=1}^{4} V_k(t, x(t), \alpha(t), \beta(t)), \tag{3.4}$$

where

$$\begin{aligned}
V_1(t, x(t), \alpha(t), \beta(t)) &= x^T(t) P_{\alpha(t)} x(t), \\
V_2(t, x(t), \alpha(t), \beta(t)) &= \int_{t-\tau_1}^{t} x^T(s) Q_1 x(s)\, ds + \int_{t-\tau(t)}^{t-\tau_1} x^T(s) Q_2 x(s)\, ds + \int_{t-\tau_2}^{t-\tau(t)} x^T(s) Q_3 x(s)\, ds, \\
V_3(t, x(t), \alpha(t), \beta(t)) &= \tau_1 \int_{t-\tau_1}^{t} \int_{v}^{t} \mathscr{F}^T(s) R_1 \mathscr{F}(s)\, ds\, dv + \tau_{12} \int_{t-\tau_2}^{t-\tau_1} \int_{v}^{t} \mathscr{F}^T(s) R_2 \mathscr{F}(s)\, ds\, dv.
\end{aligned}$$

Assume that $\alpha(t) = i$, $\alpha(t + \varsigma) = j$, $\beta(t) = \iota$ and define $\mathscr{L}$ as the weak infinitesimal operator of the stochastic process $\{x(t), \alpha(t)\}$. Then, along SES (2.6), we get

$$\mathscr{L}V_1(t, x(t), i, \iota) = 2x^T(t) P_i \mathscr{F}(t) + \mathscr{G}^T(t) P_i \mathscr{G}(t) + x^T(t) \sum_{i=1}^{N} \pi_{ij} P_j x(t)$$

$$\begin{aligned}
&= \zeta^T(t)\left[He(\varrho_1^T P_i A_{i\iota}) + \varrho_1^T\left(D_i^T P_i D_i + \tilde{P}_i\right)\varrho_1\right]\zeta(t) \\
&\quad + 2\zeta^T(t)\varrho_1^T P_i W_i \tilde{\psi}(Fx(t)) - 2\zeta^T(t)\varrho_1^T P_i K_\iota e(t) - 2\zeta^T(t)\varrho_1^T P_i E_i v(t), \qquad (3.5)\\
\mathscr{L}V_2(t, x(t), i, \iota) &= x^T(t)Q_1 x(t) + x^T(t-\tau_1)(-Q_1 + Q_2)x(t-\tau_1) \\
&\quad + (1-\dot{\tau}(t))x^T(t-\tau(t))(-Q_2 + Q_3)x(t-\tau(t)) - x^T(t-\tau_2)Q_3 x(t-\tau_2) \\
&\leqslant \zeta^T(t)\tilde{Q}\zeta(t), \qquad (3.6)\\
\mathscr{L}V_3(t, x(t), i, \iota) &= \mathscr{F}^T(t)\left(\tau_1^2 R_1 + \tau_{12}^2 R_2\right)\mathscr{F}(t) \\
&\quad - \tau_1\int_{t-\tau_1}^{t}\mathscr{F}^T(s)R_1\mathscr{F}(s)\,ds - \tau_{12}\int_{t-\tau_2}^{t-\tau_1}\mathscr{F}^T(s)R_2\mathscr{F}(s)\,ds. \qquad (3.7)
\end{aligned}$$

Define an augmented vector as $\tilde{\zeta}(t) = col\{\zeta(t), \tilde{\psi}(Fx(t)), e(t)\}$. We can derive that

$$\mathscr{F}^T(t)\left(\tau_1^2 R_1 + \tau_{12}^2 R_2\right)\mathscr{F}(t) = \begin{bmatrix}\tilde{\zeta}(t)\\ v(t)\end{bmatrix}^T \begin{bmatrix}\tilde{A}_{i\iota}^T\\ -E_i^T\end{bmatrix}\left(\tau_1^2 R_1 + \tau_{12}^2 R_2\right)\begin{bmatrix}\tilde{A}_{i\iota}^T\\ -E_i^T\end{bmatrix}^T \begin{bmatrix}\tilde{\zeta}(t)\\ v(t)\end{bmatrix}. \qquad (3.8)$$

Based on (3.1), applying Lemmas 1 and 2 to the integral terms in (3.7) yields

$$-\tau_1\int_{t-\tau_1}^{t}\mathscr{F}^T(s)R_1\mathscr{F}(s)\,ds \leqslant -\zeta^T(t)\mathcal{G}_0^T\tilde{R}_1\mathcal{G}_0\zeta(t) - 2\zeta^T(t)\mathcal{G}_0^T\tilde{R}_1\mu(t-\tau_1, t), \qquad (3.9)$$

$$-\tau_{12}\int_{t-\tau_2}^{t-\tau_1}\mathscr{F}^T(s)R_2\mathscr{F}(s)\,ds \leqslant \zeta^T(t)\left[-2\mathcal{G}_2^T S\mathcal{G}_1 - \mathcal{G}_1^T\tilde{R}_2\mathcal{G}_1 - \mathcal{G}_2^T\tilde{R}_2\mathcal{G}_2\right]\zeta(t) - 2\wp(d\varpi(t)), \qquad (3.10)$$

where $\wp(d\varpi(t)) = \frac{\tau_{12}}{\tau(t)-\tau_1}\zeta^T(t)\mathcal{G}_1^T\tilde{R}_2\mu(t-\tau(t), t-\tau_1) + \frac{\tau_{12}}{\tau_2-\tau(t)}\zeta^T(t)\mathcal{G}_2^T\tilde{R}_2\mu(t-\tau_2, t-\tau(t))$. Recalling (3.7)–(3.10), we have

$$\begin{aligned}
\mathscr{L}V_3(t, x(t), i, \iota) &\leqslant \begin{bmatrix}\tilde{\zeta}(t)\\ v(t)\end{bmatrix}^T \begin{bmatrix}\tilde{A}_{i\iota}^T\\ -E_i^T\end{bmatrix}\left(\tau_1^2 R_1 + \tau_{12}^2 R_2\right)\begin{bmatrix}\tilde{A}_{i\iota}^T\\ -E_i^T\end{bmatrix}^T \begin{bmatrix}\tilde{\zeta}(t)\\ v(t)\end{bmatrix} + \tilde{\wp}(d\varpi(t)) \\
&\quad + \zeta^T(t)\left[-\mathcal{G}_0^T\tilde{R}_1\mathcal{G}_0 - 2\mathcal{G}_2^T S\mathcal{G}_1 - \mathcal{G}_1^T\tilde{R}_2\mathcal{G}_1 - \mathcal{G}_2^T\tilde{R}_2\mathcal{G}_2\right]\zeta(t), \qquad (3.11)
\end{aligned}$$

where $\tilde{\wp}(d\varpi(t)) = -2\zeta^T(t)\mathcal{G}_0^T\tilde{R}_1\mu(t-\tau_1, t) - 2\wp(d\varpi(t))$. It follows from (2.8) that

$$-2\left(\tilde{\psi}(Fx(t)) - \acute{G}Fx(t)\right)^T L\left(\tilde{\psi}(Fx(t)) - \grave{G}Fx(t)\right) \geqslant 0,$$

which means

$$\begin{aligned}
0 &\leqslant -2\left(\tilde{\psi}(Fx(t)) - \acute{G}F\varrho_1\zeta(t)\right)^T L\left(\tilde{\psi}(Fx(t)) - \grave{G}F\varrho_1\zeta(t)\right) \\
&= -\tilde{\psi}^T(Fx(t))He(L)\tilde{\psi}(Fx(t)) + 2\zeta^T(t)\varrho_1^T F^T(\acute{G}^T + \grave{G}^T)L\tilde{\psi}(Fx(t)) \\
&\quad - \zeta^T(t)He(\varrho_1^T F^T\acute{G}^T L\grave{G}F\varrho_1)\zeta(t). \qquad (3.12)
\end{aligned}$$

In addition, recalling the adaptive ETM (2.3), we obtain

$$\begin{aligned}
0 &\leqslant \rho(t)y^T(t_k h)\Psi_i y(t_k h) - e^T(t)\Psi_i e(t) \\
&\leqslant \rho_2\left[y(t) + e(t)\right]^T\Psi_i\left[y(t) + e(t)\right] - e^T(t)\Psi_i e(t)
\end{aligned}$$

$$= \rho_2 \left[x^T(t)C_i^T\Psi_iC_ix(t) + 2x^T(t)C_i^T\Psi_ie(t) + e^T\Psi_ie(t) \right] - e^T(t)\Psi_ie(t)$$
$$= \zeta^T(t)\varrho_1^T\rho_2C_i^T\Psi_iC_i\varrho_1\zeta(t) + 2\zeta^T(t)\varrho_1^T\rho_2C_i^T\Psi_ie(t) + e^T(t)(\rho_2 - 1)\Psi_ie(t). \tag{3.13}$$

Combining (3.5), (3.6), (3.11), (3.12) and (3.13), we find that

$$\begin{aligned}\mathscr{L}V(t, x(t), i, \iota) \leqslant{}& \zeta^T(t)\Upsilon_{i\iota}^{1,1}\zeta(t) + 2\zeta^T(t)\Upsilon_i^{1,2}\tilde{\psi}(Fx(t)) + 2\zeta^T(t)\Upsilon_{i\iota}^{1,3}e(t) - 2\zeta^T(t)\varrho_1^TP_iE_iv(t)\\ &+ e^T(t)(\rho_2 - 1)\Psi_ie(t) - \tilde{\psi}^T(Fx(t))He(L)\tilde{\psi}(Fx(t)) + \tilde{\wp}(d\varpi(t)\\ &+ \begin{bmatrix} \tilde{\zeta}(t) \\ v(t) \end{bmatrix}^T \begin{bmatrix} \tilde{A}_{i\iota}^T \\ -E_i^T \end{bmatrix} \left(\tau_1^2R_1 + \tau_{12}^2R_2\right) \begin{bmatrix} \tilde{A}_{i\iota}^T \\ -E_i^T \end{bmatrix}^T \begin{bmatrix} \tilde{\zeta}(t) \\ v(t) \end{bmatrix}.\end{aligned} \tag{3.14}$$

Noting $\mathscr{E}\{\tilde{\wp}(d\varpi(t))\} = 0$, we can calculate $\mathscr{E}\{\mathscr{L}V(t, x(t), i, \iota)\}$ by (3.14) that

$$\begin{aligned}&\mathscr{E}\{\mathscr{L}V(t, x(t), i, \iota)\}\\ &\leqslant \begin{bmatrix} \tilde{\zeta}(t) \\ v(t) \end{bmatrix}^T \sum_{c=1}^{D} \varphi_{i\iota} \left(\begin{bmatrix} \Lambda_{i\iota}^{1,1} & \Lambda_i^{2,2} \\ * & 0 \end{bmatrix} + \begin{bmatrix} \tilde{A}_{i\iota}^T \\ -E_i^T \end{bmatrix} \left(\tau_1^2R_1 + \tau_{12}^2R_2\right) \begin{bmatrix} \tilde{A}_{i\iota}^T \\ -E_i^T \end{bmatrix}^T \right) \begin{bmatrix} \tilde{\zeta}(t) \\ v(t) \end{bmatrix}^T.\end{aligned} \tag{3.15}$$

Next, we discuss the SS of (2.6) under the condition of $v(t) \equiv 0$ and the LDSP of (2.6) under the condition of $v(t) \neq 0$, respectively.

i) $v(t) \equiv 0$, we can get the following inequality from (3.15):

$$\mathscr{E}\{\mathscr{L}V(t, x(t), i, \iota)\} \leqslant \tilde{\zeta}^T(t)\Lambda_i^0\tilde{\zeta}(t),$$

where $\Lambda_i^0 = \sum_{c=1}^M \varphi_{i\iota}\left(\Lambda_{i\iota}^{1,1} + \tilde{A}_{i\iota}^T\left(\tau_1^2R_1 + \tau_{12}^2R_2\right)\tilde{A}_{i\iota}\right)$. From (3.3), we can find that there exists $a > 0$ such that for any

$$\mathscr{E}\{\mathscr{L}V(t, x(t), i, \iota)\} \leqslant -a\|x(t)\|^2,\ i \in \mathscr{N}.$$

Utilizing the Itô formula, we obtain

$$\mathscr{E}\{V(t, x(t), \alpha(t))\} - \mathscr{E}\{V(0, x_0, \alpha_0)\} = \mathscr{E}\left\{\int_0^t V(s, x(s), \alpha(s))\, ds\right\} \leqslant -a\mathscr{E}\left\{\int_0^t \|x(s)\|^2\, ds\right\},$$

which means

$$\mathscr{E}\left\{\int_0^t \|x(s)\|^2\, ds\right\} \leqslant \frac{1}{a}V(0, x_0, \alpha_0).$$

Thus, the SS of (2.6) is proved.

ii) $v(t) \neq 0$, under the zero initial condition, defining $J(t) = y^T(t)y(t) - \gamma^2\int_0^t v^T(s)v(s)\, ds$ leads to

$$\begin{aligned}J(t) ={}& y^T(t)y(t) - \gamma^2\int_0^t v^T(s)v(s)\, ds + \mathscr{E}\left\{\int_0^t \mathscr{L}V(s, x(s), i, \iota)ds\right\}\\ &- (V(t, x(t), i, \iota) - V(0, x_0, \alpha_0, \beta_0))\\ \leqslant{}& x^T(t)(C_i^TC_i - P_i)x(t) + \int_0^t \begin{bmatrix} \tilde{\zeta}(s) \\ v(s) \end{bmatrix}^T \Lambda_i \begin{bmatrix} \tilde{\zeta}(s) \\ v(s) \end{bmatrix} ds.\end{aligned}$$

From conditions (3.2) and (3.3), we know that $J(t) \leqslant 0$. According to Definition 2, the SES (2.6) has a LDSP γ. □

On the basis of Theorem 1, a design method of the AAET controller can be proposed.

Theorem 2. *Given scalars ε, ρ_2 and $\gamma > 0$, suppose that there exist matrices $P_i > 0$, $Q_1 > 0$, $Q_2 > 0$, $Q_3 > 0$, $R_1 > 0$, $R_2 > 0$, $\Psi_i > 0$, diagonal matrix $L > 0$, matrices S, X_ι, Y_ι, and $T_{i\iota}$ for any $i \in \mathcal{N}$, $\iota \in \mathcal{M}$ satisfying (3.1), (3.2), and*

$$\begin{bmatrix} -He(T_{i\iota} + Y_\iota) & P_i - X_\iota - \varepsilon Y_\iota^T \\ * & -\varepsilon X_\iota - \varepsilon X_\iota^T \end{bmatrix} < 0, \tag{3.16}$$

$$\Theta_i = \sum_{c=1}^{M} \varphi_{i\iota} \begin{bmatrix} \Theta_{i\iota}^{1,1} & \Lambda_i^{1,2} & \Theta_i^{1,3} & \Theta_i^{1,4} \\ * & -\gamma^2 I & \Theta_i^{2,3} & \Theta_i^{2,4} \\ * & * & \Theta_i^{3,3} & 0 \\ * & * & * & \Theta_i^{4,4} \end{bmatrix} < 0, \tag{3.17}$$

where

$$\begin{aligned}
\Theta_{i\iota}^{1,1} &= \begin{bmatrix} \tilde{\Upsilon}_{i\iota}^{1,1} & \Upsilon_i^{1,2} & \tilde{\Upsilon}_{i\iota}^{1,3} \\ * & -He(L) & 0 \\ * & * & (\rho_2 - 1)\Psi_i \end{bmatrix}, \ \Lambda_i^{1,2} = \begin{bmatrix} -\varrho_1^T P_i E_i \\ 0 \\ 0 \end{bmatrix}, \\
\Theta_i^{1,3} &= \begin{bmatrix} \tau_1 \sqrt{\varphi_{i1}} \tilde{\aleph}_{i1}^T & \cdots & \tau_1 \sqrt{\varphi_{iM}} \tilde{\aleph}_{iM}^T \end{bmatrix}, \\
\Theta_i^{1,4} &= \begin{bmatrix} \tau_{12} \sqrt{\varphi_{i1}} \tilde{\aleph}_{i1}^T & \cdots & \tau_{12} \tilde{\aleph}_{iM}^T \end{bmatrix}, \\
\Theta_i^{2,3} &= \begin{bmatrix} -\tau_1 \sqrt{\varphi_{i1}} E_i^T P_i & \cdots & -\tau_1 \sqrt{\varphi_{iM}} E_i^T P_i \end{bmatrix}, \\
\Theta_i^{2,4} &= \begin{bmatrix} -\tau_{12} \sqrt{\varphi_{i1}} E_i^T P_i & \cdots & -\tau_{12} \sqrt{\varphi_{iM}} E_i^T P_i \end{bmatrix}, \\
\Theta_i^{3,3} &= diag\{R_1 - 2P_i, \cdots, R_1 - 2P_i\}, \ \Theta_i^{4,4} = diag\{R_2 - 2P_i, \cdots, R_2 - 2P_i\}, \\
\tilde{\Upsilon}_{i\iota}^{1,1} &= He\left(\varrho_1^T \aleph_{i\iota} - \varrho_1^T F^T \acute{G}^T L \grave{G} F \varrho_1\right) + \varrho_1^T (D_i^T P_i D_i + \tilde{P}_i)\varrho_1 \\
&\quad + \tilde{Q} - 2\mathcal{G}_2^T S \mathcal{G}_1 - \mathcal{G}_0^T \tilde{R}_1 \mathcal{G}_0 - \mathcal{G}_1^T \tilde{R}_2 \mathcal{G}_1 - \mathcal{G}_2^T \tilde{R}_2 \mathcal{G}_2 + \varrho_1^T \rho_2 C_i^T \Psi_i C_i \varrho_1, \\
\Upsilon_i^{1,2} &= \varrho_1^T P_i W_i + \varrho_1^T F^T (\acute{G}^T + \grave{G}^T) L, \ \tilde{\Upsilon}_{i\iota}^{1,3} = \varrho_1^T \rho_2 C_i^T \Psi_i + \varrho_1^T T_{i\iota}, \\
\tilde{\aleph}_{i\iota} &= \begin{bmatrix} \aleph_{i\iota} & P_i W_i & T_{i\iota} \end{bmatrix}, \ \aleph_{i\iota} = \begin{bmatrix} P_i A_i + T_{i\iota} C_i & 0 & P_i B_i & 0 & 0 & 0 & 0 \end{bmatrix}, \\
\tilde{P}_i &= \sum_{i=1}^{N} \pi_{ij} P_j, \ \tilde{R}_d = diag\{R_d, 3R_d\} \, (d = 1, 2), \\
\tilde{Q} &= diag\{Q_1, -Q_1 + Q_2, (1 - \mu_1)Q_3 - (1 - \mu_2)Q_2, -Q_3, 0_{3n \times 3n}\}, \\
\mathcal{G}_0 &= \begin{bmatrix} \varrho_1 - \varrho_2 \\ \varrho_1 + \varrho_2 - 2\varrho_5 \end{bmatrix}, \ \mathcal{G}_1 = \begin{bmatrix} \varrho_2 - \varrho_3 \\ \varrho_2 + \varrho_3 - 2\varrho_6 \end{bmatrix}, \ \mathcal{G}_2 = \begin{bmatrix} \varrho_3 - \varrho_4 \\ \varrho_3 + \varrho_4 - 2\varrho_7 \end{bmatrix}.
\end{aligned}$$

Then, AAET controller (2.5) with gains

$$K_\iota = X_\iota^{-1} Y_\iota, \ \iota \in \mathcal{M} \tag{3.18}$$

enables the SES (2.6) to have both SS and LDSP.

Proof. According to (3.18), we have $-P_i K_\iota < T_{i\iota}$ by applying Lemma 4 to (3.16). Then, we can conclude that $P_i A_{i\iota} < \aleph_{i\iota}$ and $P_i \tilde{A}_{i\iota} < \tilde{\aleph}_{i\iota}$ lead to

$$\Lambda_{i\iota}^{1,1} \leqslant \Theta_{i\iota}^{1,1}, \tag{3.19}$$

$$\Lambda_i^{1,3} \leqslant \Theta_i^{1,3}, \tag{3.20}$$

$$\Lambda_i^{1,4} \leqslant \Theta_i^{1,4}, \tag{3.21}$$

where

$$\Lambda_i^{1,3} = \begin{bmatrix} \tau_1\sqrt{\varphi_{i1}}\tilde{A}_{i1}^T P_i & \cdots & \tau_1\sqrt{\varphi_{iD}}\tilde{A}_{iD}^T P_i \end{bmatrix}, \Lambda_i^{1,4} = \begin{bmatrix} \tau_{12}\sqrt{\varphi_{i1}}\tilde{A}_{i1}^T P_i & \cdots & \tau_{12}\sqrt{\varphi_{iD}}\tilde{A}_{iD}^T P_i \end{bmatrix}.$$

Based on Lemma 3, we can get that $-P_iR_1^{-1}P_i \leqslant R_1 - 2P_i$ and $-P_iR_2^{-1}P_i \leqslant R_2 - 2P_i$, which means

$$\Lambda_i^{3,3} \leqslant \Theta_i^{3,3}, \tag{3.22}$$

$$\Lambda_i^{4,4} \leqslant \Theta_i^{4,4}, \tag{3.23}$$

where $\Lambda_i^{3,3} = diag\left\{-P_iR_1^{-1}P_i, \cdots, -P_iR_1^{-1}P_i\right\}$, $\Lambda_i^{4,4} = diag\left\{-P_iR_2^{-1}P_i, \cdots, -P_iR_2^{-1}P_i\right\}$. Due to $\varphi_{i\iota} > 0$, combining (3.19)–(3.23) yields

$$\Lambda_i^0 \leqslant \Theta_i < 0, \tag{3.24}$$

where

$$\Lambda_i^0 = \sum_{c=1}^{D} \varphi_{i\iota} \begin{bmatrix} \Lambda_{i\iota}^{1,1} & \Lambda_i^{1,2} & \Lambda_i^{1,3} & \Lambda_i^{1,4} \\ * & -\gamma^2 I & \Theta_i^{2,3} & \Theta_i^{2,4} \\ * & * & \Lambda_i^{3,3} & 0 \\ * & * & * & \Lambda_i^{4,4} \end{bmatrix}.$$

By applying Schur's complement to (3.24), we find that (3.3) can be guaranteed by (3.17). The proof is completed. □

Remark 5. *The coupling between parameter P_i and the controller gain K_ι in Theorem 1 is addressed by introducing a slack matrix $T_{i\iota}$. It is worth mentioning that directly setting the coupling term $K_\iota P_i^{-1}$ equal to the matrix $T_{i\iota}$ (i.e. $K_\iota = T_{i\iota}P_i$) would result in non-uniqueness of controller gains K_ι. In this paper, we introduce $T_{i\iota}$ such that $-P_iK_\iota < T_{i\iota}$. By designing the controller gains, as given in equation (3.18), and combining it with Lemma 4, the aforementioned issue is avoided.*

Remark 6. *Theorem 1 provides a analysis result of the SS and LDSP for SES (2.6) based on HMM, while Theorem 2 presents a design scheme for the needed AAET controller. The proofs of these theorems involve the use of the LKF in (3.4), Itô formula, as well as the inequalities in Lemmas 1-4. To further reduce the conservatism of the obtained results, one may refer to the augmented LKFs in [45, 46], the free-matrix-based approaches in [47–49], the refined CCIs in [50, 51] and the decoupling methods in [52].*

4. Simulation example

Example 1. *In this example, we consider a three-mode Chua's circuit given by*

$$\begin{cases} dx_1(t) &= [a_i(x_2(t) - m_1x_1(t) + (m_1 - m_0)\psi_1(x_1(t))) - c_ix_1(t-\tau(t))]\,dt + d_i(x_2(t) - m_1x_1(t))\,d\varpi(t), \\ dx_2(t) &= [x_1(t) - x_2(t) + x_3(t) - c_ix_1(t-\tau(t))]\,dt + 0.1\,(x_1(t) - x_2(t) + x_3(t))\,d\varpi(t), \\ dx_3(t) &= [-b_ix_2(t) + c_i(2x_1(t-\tau(t)) - x_3(t-\tau(t)))]\,dt - m_3x_2(t)d\varpi(t), \end{cases}$$

where parameters $m_0 = -\frac{1}{7}$, $m_1 = \frac{2}{7}$, $m_3 = 0.1$, *and* a_i, b_i, c_i, d_i $(i = 1, 2, 3)$ *are listed in Table 1. The nonlinear characteristics* $\psi_1(x_1(t)) = \frac{1}{2}(|x_1(t) + 1| - |x_1(t) - 1|)$ *belonging to sector* $[0, 1]$, *and* $\psi_2(x_2(t)) = \psi_3(x_3(t)) = 0$. *The circuit model can be re-expressed as LS (2.1) with*

$$A_i = \begin{bmatrix} -a_i m_1 & a_i & 0 \\ 1 & -1 & 1 \\ 0 & -b_i & 0 \end{bmatrix}, B_i = \begin{bmatrix} -c_i & 0 & 0 \\ -c_i & 0 & 0 \\ 2c_i & 0 & -c_i \end{bmatrix},$$

$$D_i = \begin{bmatrix} -d_i m_1 & d_i & 0 \\ 0.1 & -0.1 & 0.1 \\ 0 & -m_3 & 0 \end{bmatrix}, C_i = \begin{bmatrix} -1 & 0 & 0 \\ 0 & -1 & 0 \\ 0 & 0 & -1 \end{bmatrix},$$

$$W_i = \begin{bmatrix} a_i(m_1 - m_0) & 0 & 0 \\ 0 & 0 & 0 \\ 0 & 0 & 0 \end{bmatrix}, E_i = \begin{bmatrix} 0.1 & 0 & 0 \end{bmatrix}^T.$$

Table 1. The parameters a_i, b_i, c_i, d_i in the Chua's circuit.

i	a_i	b_i	c_i	d_i
1	9	14.28	0.1	0.01
2	8	10	0.05	0.01
3	9	14	0.15	0.01

The delay parameters are specified as $\tau_1 = 0.1$, $\tau_2 = 0.18$, $\mu_1 = 0.1$ *and* $\mu_2 = 0.26$, *the parameters related to the adaptive law are given by* $\rho_1 = 0.1$, $\rho_2 = 0.9$, $\kappa = 0.5$ *and the TR and CTP matrices are chosen as*

$$\Pi = \begin{bmatrix} -5 & 2 & 3 \\ 3 & -6 & 3 \\ 4 & 1 & -5 \end{bmatrix}, \Phi = \begin{bmatrix} 0.4 & 0.3 & 0.3 \\ 0.2 & 0.3 & 0.5 \\ 0.4 & 0.5 & 0.1 \end{bmatrix}.$$

By solving the LMIs in Theorem 2, the optimal LDSP is found to be $\gamma^* = 0.0553$, *and the controller gains and adaptive ETM weight matrices are calculated as*

$$K_1 = \begin{bmatrix} -2.1803 & -3.4217 & -0.2840 \\ -0.3775 & -0.1768 & 0.0748 \\ 0.2038 & -1.8311 & -2.1877 \end{bmatrix}, K_2 = \begin{bmatrix} -2.1223 & -3.3641 & -0.3704 \\ -0.4417 & -0.4562 & -0.0072 \\ 0.2660 & -0.9016 & -2.0248 \end{bmatrix},$$

$$K_3 = \begin{bmatrix} -2.1969 & -2.9252 & -0.3438 \\ -0.4544 & -0.0631 & 0.0453 \\ 0.2441 & -1.2244 & -2.1906 \end{bmatrix}, \Psi_1 = \begin{bmatrix} 12.3581 & 6.0393 & -0.0059 \\ 6.0393 & 24.5561 & 5.5930 \\ -0.0059 & 5.5930 & 12.6577 \end{bmatrix},$$

$$\Psi_2 = \begin{bmatrix} 12.3187 & 9.0377 & 1.0279 \\ 9.0377 & 22.2312 & 4.1752 \\ 1.0279 & 4.1752 & 12.0248 \end{bmatrix}, \Psi_3 = \begin{bmatrix} 12.0007 & 9.9128 & 0.6669 \\ 9.9128 & 24.4770 & 4.4405 \\ 0.6669 & 4.4405 & 12.1092 \end{bmatrix}.$$

We set the initial states as $x_m(t) = \begin{bmatrix} -0.2 & -0.3 & 0.2 \end{bmatrix}^T$, $x_s(t) = \begin{bmatrix} 0.25 & 0.35 & 0.35 \end{bmatrix}^T$ $(t \in [-\tau_2, 0])$ *and the disturbance as* $v(t) = 0.1 sint(t)$. *The sampling period is chosen to be* $h = 0.05s$. *A possible* *mode evolution of system and AAET controller is drawn in Figure 2. When there is no controller applied, we can find from Figure 3 that the system is unstable. By utilizing the devised AAET controller shown in Figure 4, the state response curves of the SES (2.6) are exhibited in Figure 5. It can be seen that the synchronization error between the master and slave LSs approaches zero over time, indicating that the master and slave LSs can successfully achieve synchronization under the presented AAET controller. The trajectory of the adaptive law and release time intervals between two trigger moments are depicted in Figures 6 and 7, respectively. Based on the simulation results, it can be observed that as the SES (2.6) stabilizes, the threshold function gradually converges to a fixed value. Define the function* $\gamma(t) = \sqrt{\mathscr{E}\left\{\sup_{t\geqslant 0}\{\|y(t)\|^2\}\right\} / \mathscr{E}\left\{\int_0^t \|v(s)\|^2 ds\right\}}$ *for LDSP. Then the trajectory of* $\gamma(t)$ *under zero initial condition is depicted in Figure 8. It is evident from Figure 8 that the maximum value of* $\gamma(t)$ *is* 0.0047, *which is lower than* $\gamma^* = 0.0553$.

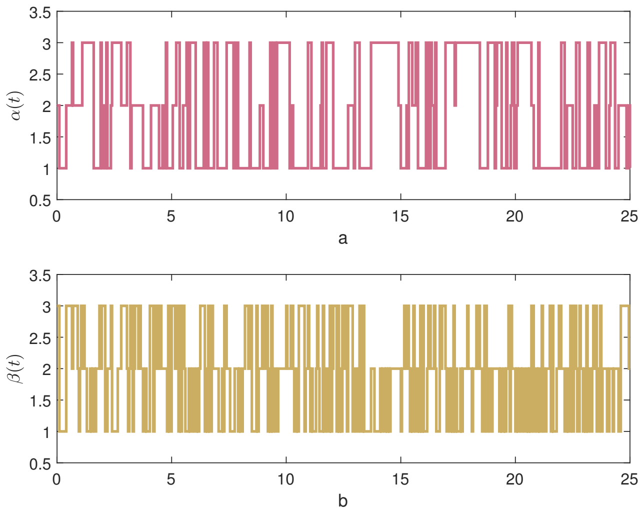

Figure 2. Possible mode evolution processes of the LSs and AAET controller.

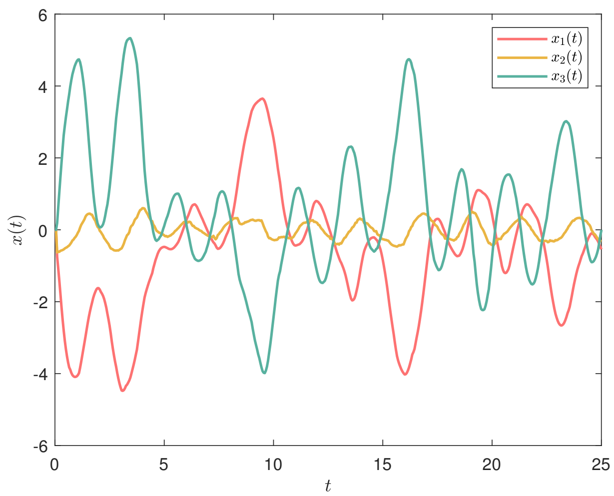

Figure 3. Trajectory of SES (2.6) without control.

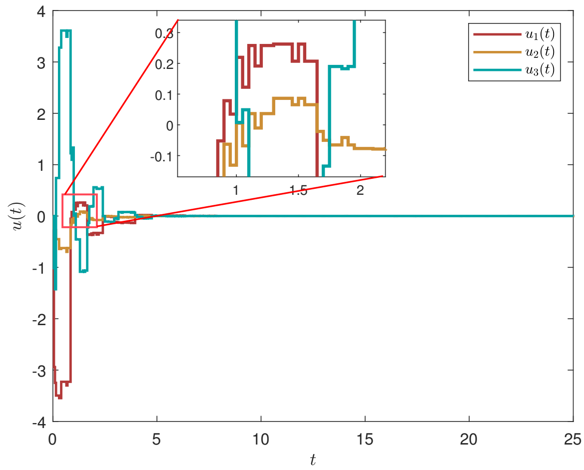

Figure 4. Trajectory of AAET controller (2.5).

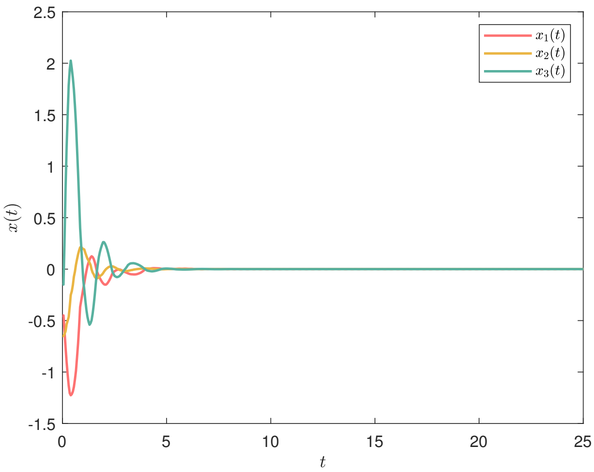

Figure 5. Trajectory of SES (2.6) with control.

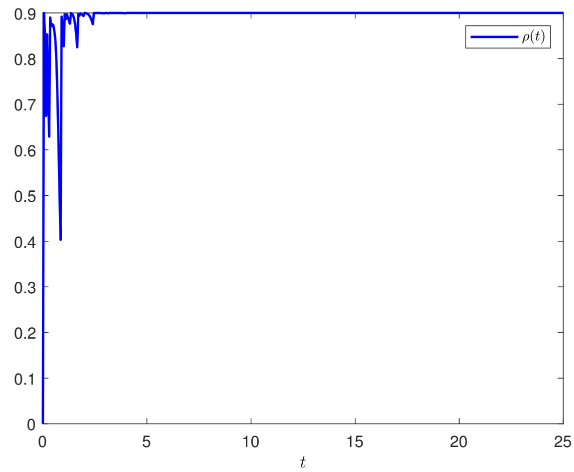

Figure 6. Trajectory of the adaptive law.

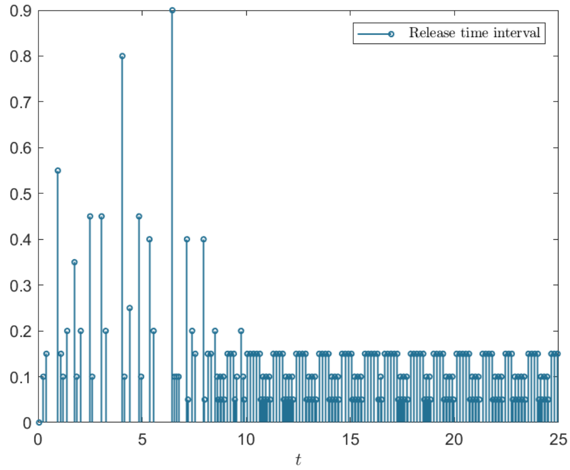

Figure 7. Release time intervals.

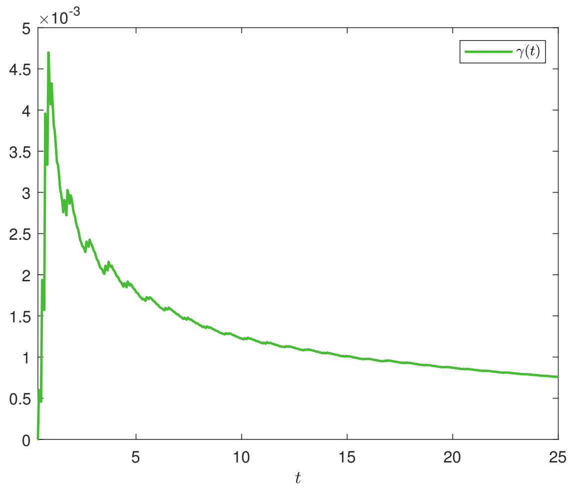

Figure 8. Trajectory of $\gamma(t)$

Table 2 presents the data transmission rates under different triggering mechanisms in the same conditions. The comparison demonstrates that the adaptive ETM employed in this study can effectively reduce data transmission to achieve the goal of conserving channel resources.

Table 2. The data transmission rates under different triggering mechanisms.

	SDM in [14]	PETM in [53]	Adaptive ETM in this paper
Number of transmitted data	500	236	194
Data transmission rates	100%	47.20%	38.80%

5. Conclusions

The master-slave chaos synchronization of stochastic time-delay LSs (2.1) and (2.2) within a networked environment has been considered. To tackle the challenges posed by potential mode-mismatch behavior and limited networked channel resources, the AAET controller in (2.5) has been employed. A criterion on the SS and LDSP of the SES (2.6) has been proposed in Theorem 1 using a LKF, a Wirtinger-type inequality, the Itô formula, as well as a CCI. Then, a method for determining the desired AAET controller gains has been proposed in Theorem 2 by decoupling the nonlinearities that arise from the Lyapunov matrices and controller gains. Finally, simulation results have confirmed that the designed controller can achieve chaos synchronization between the master LS (2.1) and slave LS (2.2), while significantly reducing data transmission.

Use of AI tools declaration

The authors declare they have not used Artificial Intelligence (AI) tools in the creation of this article.

Acknowledgments

This work was supported by the Key Research and Development Project of Anhui Province (Grant No. 202004a07020028).

Conflict of interest

All authors declare no conflicts of interest in this paper.

References

1. L. O. Chua, L. Kocarev, K. Eckert, M. Itoh, Experimental chaos synchronization in Chua's circuit, *Int. J. Bifurcat. Chaos*, **2** (1992), 705–708. https://doi.org/10.1142/S0218127492000811
2. H. Sompolinsky, A. Crisanti, H. J. Sommers, Chaos in random neural networks, *Phys. Rev. Lett.*, **61** (1988), 259. https://doi.org/10.1103/PhysRevLett.61.259
3. J. A. K. Suykens, A. Huang, L. O. Chua, A family of n-scroll attractors from a generalized Chua's circuit, *AEU Int. J. Electron. Commun.*, **51** (1997), 131–137.
4. Y. Fan, Z. Wang, X. Huang, H. Shen, Using partial sampled-data information for synchronization of chaotic Lur'e systems and its applications: an interval-dependent functional method, *Inform. Sci.*, **619** (2023), 358–373. https://doi.org/10.1016/j.ins.2022.11.066
5. L. Wang, S. Jiang, M. F. Ge, C. Hu, J. Hu, Finite-/fixed-time synchronization of memristor chaotic systems and image encryption application, *IEEE Trans. Circuits-I*, **68** (2021), 4957–4969. https://doi.org/10.1109/TCSI.2021.3121555
6. S. Moon, J. J. Baik, J. M. Seo, Chaos synchronization in generalized Lorenz systems and an application to image encryption, *Commun. Nonlinear Sci.*, **96** (2021), 105708. https://doi.org/10.1016/j.cnsns.2021.105708
7. M. Roohi, C. Zhang, Y. Chen, Adaptive model-free synchronization of different fractional-order neural networks with an application in cryptography, *Nonlinear Dyn.*, **100** (2020), 3979–4001. https://doi.org/10.1007/s11071-020-05719-y

8. V. K. Yadav, V. K. Shukla, S. Das, Exponential synchronization of fractional-order complex chaotic systems and its application, *Chaos Solitons Fractals*, **147** (2021), 110937. https://doi.org/10.1016/j.chaos.2021.110937

9. S. Lakshmanan, M. Prakash, C. P. Lim, R. Rakkiyappan, P. Balasubramaniam, S. Nahavandi, Synchronization of an inertial neural network with time-varying delays and its application to secure communication, *IEEE Trans. Neural Net. Learn. Syst.*, **29** (2018), 195–207. https://doi.org/10.1109/TNNLS.2016.2619345

10. A. M. Gonzalez-Zapata, E. Tlelo-Cuautle, I. Cruz-Vega, W. D. León-Salas, Synchronization of chaotic artificial neurons and its application to secure image transmission under MQTT for IoT protocol, *Nonlinear Dyn.*, **104** (2021), 4581–4600. https://doi.org/10.1007/s11071-021-06532-x

11. W. Shao, Y. Fu, M. Cheng, L. Deng, D. Liu, Chaos synchronization based on hybrid entropy sources and applications to secure communication, *IEEE Photonic. Tech. Lett.*, **33** (2021), 1038–1041. https://doi.org/10.1109/LPT.2021.3093584

12. Q. Li, X. Liu, Q. Zhu, S. Zhong, J. Cheng, Stochastic synchronization of semi-Markovian jump chaotic Lur'e systems with packet dropouts subject to multiple sampling periods, *J. Franklin I.*, **356** (2019), 6899–6925. https://doi.org/10.1016/j.jfranklin.2019.06.005

13. Y. Li, J. Feng, J. Wang, Mean square synchronization for stochastic delayed neural networks via pinning impulsive control, *Electron. Res. Arch.*, **30** (2022), 3172–3192. http://dx.doi.org/10.3934/era.2022161

14. T. Yang, Z. Wang, J. Xia, H. Shen, Sampled-data exponential synchronization of stochastic chaotic Lur'e delayed systems, *Math. Comput. Simulation*, **203** (2023), 44–57. https://doi.org/10.1016/j.matcom.2022.06.010

15. Y. Zhou, X. H. Chang, W. Huang, Z. M. Li, Quantized extended dissipative synchronization for semi-Markov switching Lur'e systems with time delay under deception attacks, *Commun. Nonlinear Sci.*, **117** (2023), 106972. https://doi.org/10.1016/j.cnsns.2022.106972

16. X. H. Chang, Y. Liu, Quantized output feedback control of AFS for electric vehicles with transmission delay and data dropouts, *IEEE Trans. Intell. Transp. Syst.*, **23** (2022), 16026–16037. https://doi.org/10.1109/TITS.2022.3147481

17. C. Jia, J. Hu, H. Liu, J. Du, S. Feng, Recursive state estimation for a class of nonlinear uncertain coupled complex networks subject to random link failures and packet disorders, *ISA Trans.*, **127** (2022), 88–98. https://doi.org/10.1016/j.isatra.2021.12.036

18. D. Xu, X. Li, W. Tai, J. Zhou, Event-triggered stabilization for networked control systems under random occurring deception attacks, *Math. Biosci. Eng.*, **20** (2023), 859–878. http://dx.doi.org/10.3934/mbe.2023039

19. J. Zhou, D. Xu, W. Tai, C. K. Ahn, Switched event-triggered $\mathcal{H}_\infty$ security control for networked systems vulnerable to aperiodic DoS attacks, *IEEE Trans. Net. Sci. Eng.*, **10** (2023), 2109–2123. https://doi.org/10.1109/TNSE.2023.3243095

20. Y. Fan, X. Huang, Y. Li, H. Shen, Sampled-data-based secure synchronization control for chaotic Lur'e systems subject to Denial-of-Service attacks, *IEEE Trans. Neural Net. Learn. Syst.*, **2022** (2022). https://doi.org/10.1109/TNNLS.2022.3203382

21. Y. Xu, Z. G. Wu, Y. J. Pan, J. Sun, Resilient asynchronous state estimation for Markovian jump neural networks subject to stochastic nonlinearities and sensor saturations, *IEEE Trans. Cybern.*, **52** (2022), 5809–5818. https://doi.org/10.1109/TCYB.2020.3042473

22. L. R. Rabiner, A tutorial on hidden Markov models and selected applications in speech recognition, *Proc. IEEE*, **77** (1989), 257–286. https://doi.org/10.1109/5.18626

23. F. Li, S. Song, J. Zhao, S. Xu, Z. Zhang, Synchronization control for Markov jump neural networks subject to HMM observation and partially known detection probabilities, *Appl. Math. Comput.*, **360** (2019), 1–13. https://doi.org/10.1016/j.amc.2019.04.032

24. C. Ma, L. Hao,H. Fu, Neural network based asynchronous synchronization for fuzzy hidden Markov jump complex dynamical networks, *Complex Intell. Syst.*, **8** (2022), 1941–1948. https://doi.org/10.1007/s40747-021-00370-5

25. W. Wu, L. He, J. Zhou, Z. Xuan, S. Arik, Disturbance-term-based switching event-triggered synchronization control of chaotic Lurie systems subject to a joint performance guarantee, *Commun. Nonlinear Sci.*, **115** (2022), 106774. https://doi.org/10.1016/j.cnsns.2022.106774

26. W. He, T. Luo, Y. Tang, W. Du, Y. C. Tian, F. Qian, Secure communication based on quantized synchronization of chaotic neural networks under an event-triggered strategy, *IEEE Trans. Neural Net. Learn. Syst.*, **31** (2020), 3334–3345. https://doi.org/10.1109/TNNLS.2019.2943548

27. Y. Ni, Z. Wang, Y. Fan, X. Huang, H. Shen, Memory-based event-triggered control for global synchronization of chaotic Lur'e systems and its application, *IEEE Trans. Syst. Man Cybern. Syst.*, **53** (2023), 1920–1931. https://doi.org/10.1109/TSMC.2022.3207353

28. Y. Ni, Z. Wang, Y. Fan, J. Lu, H. Shen, A switching memory-based event-trigger scheme for synchronization of Lur'e systems with actuator saturation: A hybrid Lyapunov method, *IEEE Trans. Neural Net. Learn. Syst.*, 2023. https://doi.org/10.1109/TNNLS.2023.3273917

29. Z. Gu, S. Yan, J. H. Park, X. Xie, Event-triggered synchronization of chaotic Lur'e systems via memory-based triggering approach, *IEEE Trans. Circuits-II*, **69** (2022), 1427–1431. https://doi.org/10.1109/TCSII.2021.3113955

30. W. Tai, D. Zuo, Z. Xuan, J. Zhou, Z. Wang, Non-fragile $\mathcal{L}_2 - \mathcal{L}_\infty$ filtering for a class of switched neural networks, *Math. Comput. Simulation*, **185** (2021), 629–645. https://doi.org/10.1016/j.matcom.2021.01.014

31. P. Selvaraj, O. Kwon, S. Lee, R. Sakthivel, Robust fault-tolerant control design for polynomial fuzzy systems, *Fuzzy Sets Syst.*, **464** (2023), 108406. https://doi.org/10.1016/j.fss.2022.09.012

32. X. Li, X. Ma, W. Tai, J. Zhou, Designing an event-triggered $\mathcal{H}_\infty$ filter with possibly inconsistent modes for Markov jump systems, *Digital Signal Process.*, **139** (2023), 104092. https://doi.org/10.1016/j.dsp.2023.104092

33. J. Gu, H. Wang, W. Li, Output-feedback stabilization for stochastic nonlinear systems with Markovian switching and time-varying powers, *Math. Biosci. Eng.*, **19** (2022), 11071–11085. http://dx.doi.org/10.3934/mbe.2022516

34. W. Tai, X. Li, J. Zhou, S. Arik, Asynchronous dissipative stabilization for stochastic Markov-switching neural networks with completely-and incompletely-known transition rates, *Neural Net.*, **161** (2023), 55–64. https://doi.org/10.1016/j.neunet.2023.01.039

35. R. Vadivel, P. Hammachukiattikul, N. Gunasekaran, R. Saravanakumar, H. Dutta, Strict dissipativity synchronization for delayed static neural networks: An event-triggered scheme, *Chaos Solitons Fractals*, **150** (2021), 111212. https://doi.org/10.1016/j.chaos.2021.111212

36. X. Liu, K. Shi, Y. Tang, L. Tang, Y. Wei, Y. Han, A novel adaptive event-triggered reliable $\mathcal{H}_\infty$ control approach for networked control systems with actuator faults, *Electron. Res. Arch.*, **31** (2023), 1840–1862. http://dx.doi.org/10.3934/era.2023095

37. L. Yao, X. Huang, Memory-based adaptive event-triggered secure control of Markovian jumping neural networks suffering from deception attacks, *Sci. China Technol. Sci.*, **66** (2023), 468–480. https://doi.org/10.1007/s11431-022-2173-7

38. J. Zhou, J. Dong, S. Xu, Asynchronous dissipative control of discrete-time fuzzy Markov jump systems with dynamic state and input quantization, *IEEE Trans. Fuzzy Syst.*, 2023. https://doi.org/10.1109/TFUZZ.2023.3271348

39. S. Dong, M. Liu, Adaptive fuzzy asynchronous control for nonhomogeneous Markov jump power systems under hybrid attacks, *IEEE Trans. Fuzzy Syst.*, **31** (2023), 1009–1019. https://doi.org/10.1109/TFUZZ.2022.3193805

40. J. Wang, X. M. Zhang, Y. Lin, X. Ge, Q. L. Han, Event-triggered dissipative control for networked stochastic systems under non-uniform sampling, *Inform. Sci.*, **447** (2018), 216–228. https://doi.org/10.1016/j.ins.2018.03.003

41. F. Zeng, Y. Wang, G. Zhuang, F. Chen, Dynamic-memory event-triggered-based controller design for singular stochastic semi-Markov jump systems against multiple cyber-attacks, *Nonlinear Dyn.*, **110** (2022), 1559–1582. https://doi.org/10.1007/s11071-022-07728-5

42. E. K. Boukas, *Control of singular systems with random abrupt changes*, Springer, Berlin, 2008.

43. X. H. Chang, J. H. Park, J. Zhou, Robust static output feedback $\mathcal{H}_\infty$ control design for linear systems with polytopic uncertainties, *Syst. Control Lett.*, **85** (2015), 23–32. https://doi.org/10.1016/j.sysconle.2015.08.007

44. I. Kucukdemiral, X. Han, M. S. Erden, Robust induced $l_2 - l_\infty$ optimal control of discrete-time systems having magnitude and rate-bounded actuators, *ISA Trans.*, **129** (2022), 73–87. https://doi.org/10.1016/j.isatra.2022.02.025

45. H. B. Zeng, Z. L. Zhai, Y. He, K. L. Teo, W. Wang, New insights on stability of sampled-data systems with time-delay, *Appl. Math. Comput.*, **374** (2020), 125041. https://doi.org/10.1016/j.amc.2020.125041

46. T. S. Peng, H. B. Zeng, W. Wang, X. M. Zhang, X. G. Liu, General and less conservative criteria on stability and stabilization of T–S fuzzy systems with time-varying delay, *IEEE Trans. Fuzzy Syst.*, **31** (2023), 1531–1541. https://doi.org/10.1109/TFUZZ.2022.3204899

47. W. Wang, H. B. Zeng, K. L. Teo, Y. J. Chen, Relaxed stability criteria of time-varying delay systems via delay-derivative-dependent slack matrices, *J. Franklin I.*, **360** (2023), 6099–6109. https://doi.org/10.1016/j.jfranklin.2023.04.019

48. H. B. Zeng, Y. He, M. Wu, J. She, New results on stability analysis for systems with discrete distributed delay, *Automatica*, **60** (2015), 189–192. https://doi.org/10.1016/j.automatica.2015.07.017

49. H. B. Zeng, X. G. Liu, W. Wang, A generalized free-matrix-based integral inequality for stability analysis of time-varying delay systems, *Appl. Math. Comput.*, **354** (2019), 1–8. https://doi.org/10.1016/j.amc.2019.02.009
50. H. B. Zeng, H. C. Lin, Y. He, K. L. Teo, W. Wang, Hierarchical stability conditions for time-varying delay systems via an extended reciprocally convex quadratic inequality, *J. Franklin I.*, **357** (2020), 9930–9941. https://doi.org/10.1016/j.jfranklin.2020.07.034
51. H. C. Lin, H. B. Zeng, X. M. Zhang, W. Wang, Stability analysis for delayed neural networks via a generalized reciprocally convex inequality, *IEEE Trans. Neural Net. Learn. Syst.*, 2022. https://doi.org/10.1109/TNNLS.2022.3144032
52. W. Wang, H. B. Zeng, A looped functional method to design state feedback controllers for Lurie networked control systems, *IEEE/CAA J. Autom. Sinica*, **10** (2023), 1093–1095. https://doi.org/10.1109/JAS.2023.123141
53. E. Tian, C. Peng, Memory-based event-triggering $\mathcal{H}_\infty$ load frequency control for power systems under deception attacks, *IEEE Trans. Cybern.*, **50** (2020), 4610–4618. https://doi.org/10.1109/TCYB.2020.2972384